Influence of Process Pressure on Local Facesheet Instability for Ultra-light Sandwich Structures

JULIEN RION, SAMUEL STUTZ, YVES LETERRIER*
AND JAN-ANDERS E. MÅNSON
Laboratoire de Technologie des Composites et Polymères (LTC), Ecole Polytechnique Fédérale de Lausanne (EPFL), CH-1015 Lausanne, Switzerland

ABSTRACT: Skin wrinkling phenomenon is investigated in the case of ultra-light sandwich structures with a honeycomb core manufactured by one-shot vacuum bag processing. The interplay between process pressure and compressive strength of the skin is established. It is observed that the size of the adhesive menisci between honeycomb cell walls and skin, and the waviness of the skin increases with process pressure. As these two effects exert opposing influences on the compressive strength of the skin, an optimal process pressure equal to 0.7 bar is identified experimentally and confirmed by an analytical model.

KEY WORDS: wrinkling, honeycomb core, facesheet waviness, process pressure, adhesive menisci.

INTRODUCTION

COMPOSITE SANDWICH STRUCTURES are very often used for all applications requiring high stiffness and strength with minimal weight [1–4]. High-tech applications, such as satellites, ultra-light solar airplanes [5–7] or solar cars, require pushing this type of structure to the limit in terms of lightness. To this end, sandwich structures with very thin skins and light honeycomb core weighing $<1\,kg/m^2$ are used. While traditional sandwich structures used in boat hulls or commercial airplanes have often been studied and optimized (e.g., [8,9]), ultra-light sandwich structures require particular attention in their design and manufacture. In fact, these structures are extremely sensitive to local buckling of their very thin skins, either

*Author to whom the correspondence should be addressed. E-mail: yves.leterrier@epfl.ch
Figures 1, 3, 4, 6, 7 and 10–13 appear in color online: http://jsm.sagepub.com

1099-6362/09/04 0293–19 $10.00/0 DOI: 10.1177/1099636209104513

through wrinkling or dimpling [10–12]. Wrinkling was already studied in 1950 by Norris et al. [13], Hoff and Mautner [14], and Yusuff [15] and numerous models have been developed since. Ley et al. [10] made an extensive review of the most commonly used wrinkling models and compared it to experimental results. They found that a main limitation of the models was due to the fact that this failure mode is very sensitive to local imperfections of the skin, which can dramatically reduce the strength of the structure. These local imperfections were taken into account by Kassapoglou et al. [16], who considered an initial sinusoidal waviness of the skin combined with Hoff's model to predict wrinkling failure. However, the amplitude of initial imperfection was arbitrarily fixed to match the experimental results. Similarly, more recently, Fagerberg and Zenkert [17] used Allen's model [18] combined with initial sinusoidal waviness of the skin to predict imperfections induced wrinkling in foam core sandwiches. They obtained a good prediction of failure loads assuming small initial imperfections in the skin between 0.01 and 0.25 mm.

Thus the processing of ultralight sandwich panels needs to be studied very carefully in order to minimize any local irregularities in the skins. Particularly, during one-shot manufacturing of sandwich panels by vacuum bag processing, the facesheet on the vacuum bag side presents waviness due to penetration of the skin into honeycomb cells [16,19,20]. This phenomenon significantly decreases the strength of the sandwich panel when the skin is under compressive loads. As skin waviness is dependent on the level of vacuum applied during curing, the relation between processing pressure, (i.e., the difference between atmospheric pressure and pressure in the vacuum bag), and wrinkling load was studied in order to determine the optimal process conditions. Therefore, the wrinkling model developed by Gutierrez and Weber [21], which is adapted to sandwiches with honeycomb core in bending, was used considering an initial sinusoidal waviness of the skin. Its amplitude was related to the process pressure.

In addition, the process pressure changes not only the waviness of the skin, but was also expected to influence the formation of the adhesive menisci between honeycomb cell walls and skins. The relation between the amount of adhesive in the menisci and the wrinkling load was therefore considered first.

MATERIALS AND METHODS

Three different kinds of ultralight sandwich structures were fabricated to evaluate the interplay between process pressure, waviness of the skin, adhesive weight in menisci, and failure load of the skin. All the samples were produced using the same materials and their weight ranged from 700 to 800 g/m^2.

The skins comprised two layers of 70 g/m^2 UD carbon fiber prepreg with an EH84 epoxy matrix (Hexcel) at 0 and 90°, respectively. The Nomex® honeycomb core was 29 kg/m^3 and the hexagonal cell size, i.e., the distance between two parallel cell walls was 3.2 mm. The core was 8 mm thick. The ribbon direction of the honeycomb was parallel to the lengthwise direction of the sandwich panel. An epoxy adhesive (VTA 260 from Advanced Composite Group) was used to bond the skins to the core.

The first samples were prepared in order to study the effect of adhesive weight in the resin menisci on the compressive failure load of the skin. The sandwich samples were fabricated in one shot by the vacuum bag process. As, during one-shot curing, the skin on the vacuum bag side had a lower quality due to waviness, the study concentrated on the smooth skin on the mold side. The effect of waviness of the skin on the vacuum bag side was considered in other samples. Five different adhesive weights between 0 (no supplementary adhesive was used) and 100 g/m^2 were chosen for the smooth side by using the adhesive deposition method developed by Rion et al. [22,23]. The complete panel was cured under vacuum (−0.9 bar relative pressure) at 120°C during 100 min. An Al frame prevented lateral crushing when vacuum was applied, as illustrated in Figure 1. A non-perforated film was placed on top of the prepreg to prevent resin flowing out of the prepreg. Fiber rovings were placed between the Al frame and the non-perforated film to enable air to circulate. As the film prevented air circulation through the thickness of the skin, the vacuum was only applied from the sides of the panels and a good vacuum could not be ensured in the honeycomb cells.

The second type of samples was produced to study the influence of processing pressure on the strength of the panel. To allow the vacuum level in the honeycomb cells during curing to be controlled, the panels were processed in two steps. The wavy skin was fabricated first. The honeycomb was laid onto a plate with a breather cloth in-between thereby channeling air under the honeycomb. The adhesive film and carbon prepreg were then laid onto the honeycomb and finally the consumables were stacked as described in Figure 1. Although the breather cloth and plastic grid on top of the panel were not useful for draining air during the first cure, because the air was drained below the honeycomb, it was nevertheless included in order to have the same stacking on the surface as for conventional one-shot vacuum processing. Five different relative vacuum pressures (i.e., $P_v - P_{atm}$, where P_v is the absolute pressure in vacuum bag, and P_{atm} is the atmospheric pressure) were used: −0.1, −0.3, −0.5, −0.7, −0.9 bar. In a second step, the second skin was laid on the Al plate, the honeycomb with the first skin already cured was placed on it with all the consumables and it was cured with −0.9 bar relative vacuum pressure. The vacuum was applied during 5 h before the second curing cycle began to allow air to circulate in order to

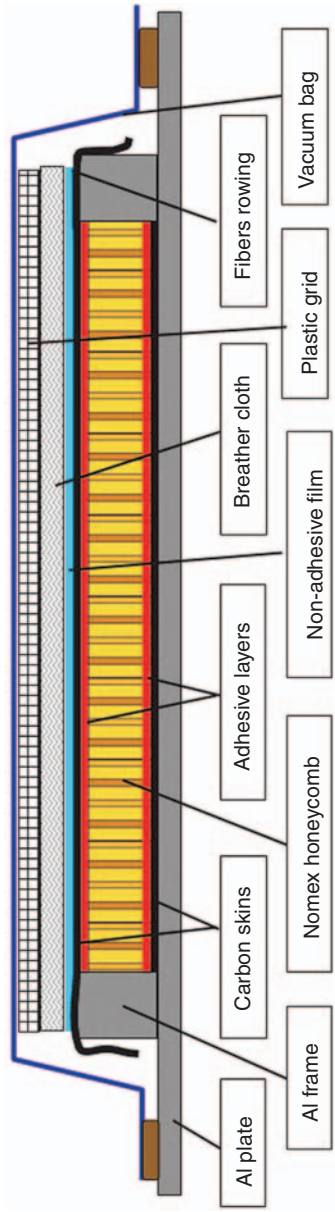

Figure 1. *Vacuum processing layout of the sandwich panels cured in one shot.*

create a vacuum in the honeycomb cells. A 50 g/m^2 adhesive film was used to bond both skins to the core.

The third type of samples was fabricated with the same lay-up and adhesive quantity as the second type, but in one shot. Various relative vacuum pressures (−0.1, −0.5, −0.7, −0.9 bar) were used, as for the second type of samples, but as the honeycomb cells were closed on both sides by the carbon skins during curing, so the absolute pressure in the honeycomb cells could be considerably higher than that obtained under the vacuum bag. The vacuum was applied during 12 h before the curing cycle began to allow air circulation.

Using a diamond saw, the panels were cut into seven samples of 30 mm width and 450 mm length and tested in four-point bending. The span between the outer supports in four-point loading was 400 mm, and 100 mm between the loading points. Small carbon plates of 18 mm width and 1.5 mm thickness were placed under the loading points to avoid local indentation.

The waviness W_{meas} of the skin was measured on micrographs of polished cross-sections of the sandwich structures. Figure 2 shows the measured waviness, i.e., the height difference between the top of honeycomb cells and the lower point of the skin in the middle of the honeycomb cell. The size of the adhesive menisci between honeycomb cell walls and the carbon skin was also measured on the polished cross-sections, and the weight of adhesive in the menisci was calculated according to a geometrical model of the menisci [23]. This model is based on the contact angles formed by the adhesive on the CFRP facesheet and on the Nomex honeycomb cell walls.

To calculate the wrinkling load of the skin under compression, the bending stiffness of the facesheet had to be known accurately. Therefore, after testing the sandwich beams in four-point bending, a 90 mm length of skin was cut from the smooth side of the beams. The honeycomb was removed from the skin by cutting it with a cutter at the top of the adhesive menisci (Figure 3). The stiffness of the skin reinforced by the adhesive menisci was measured in a three-point bending test, with a span of 50 mm.

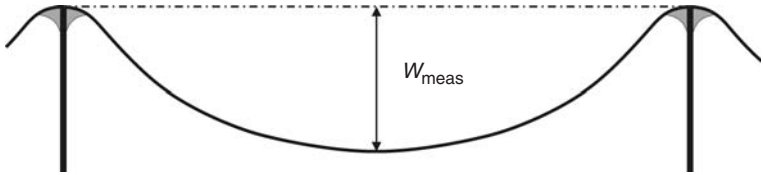

Figure 2. *Measurement of the amplitude of the waviness on the micrographs of cross-sections.*

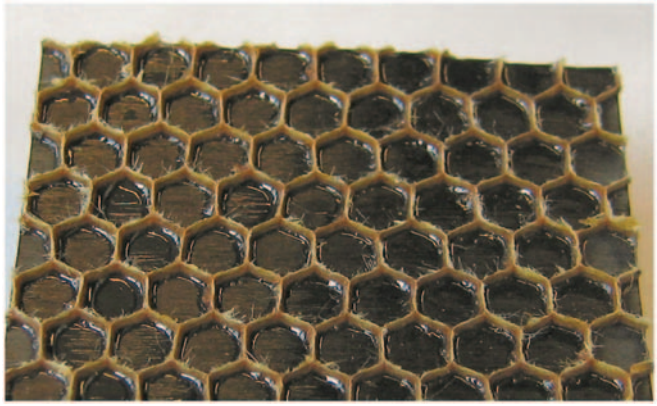

Figure 3. *CFRP skin with adhesive menisci on the surface.*

MODELING OF WRINKLING PHENOMENON

As all the samples tested in four-point bending broke, due to wrinkling of the skin under compression between the two loading points, as illustrated in Figure 4, this particular failure mode was investigated. The wrinkling problem has been extensively studied by numerous authors. Ley et al. [10] reviewed the most commonly used models. All the models are based on the same assumption of compressed skin laying on a continuous elastic foundation. The main difference between the various models is the modeling of the elastic foundation according to the core used. When honeycomb core is used, the anti-plane stress assumption is often used, i.e., the core is considered to have an in-plane stiffness of zero, and so to have only normal stresses perpendicular to the panel, and shear stresses in zx- and zy-planes, where z is perpendicular to the panel. The model proposed by Gutierrez and Webber [21], which was especially developed for bending sandwich panels, used this assumption and was thus well adapted to the case studied in the present paper. This model also took into account the elastic tension–bending coupling in asymmetric composite skins. In fact, as it was observed that taking coupling into account changed the wrinkling load by <1% in the present case, this was disregarded in order to simplify the study. This simplification can only be done when symmetrical or thin facesheets with low tension–bending coupling loads are used. The equilibrium equations for the skin under a compressive load, as represented in Figure 5 are then

$$A\frac{\mathrm{d}^2 u_\mathrm{f}}{\mathrm{d}x^2} = (\tau_{xz})_{z=d_s} \quad -D\frac{\mathrm{d}^4 w_\mathrm{f}}{\mathrm{d}x^4} - N\frac{\mathrm{d}^2 w_\mathrm{f}}{\mathrm{d}x^2} = (\sigma_z)_{z=d_s} \tag{1}$$

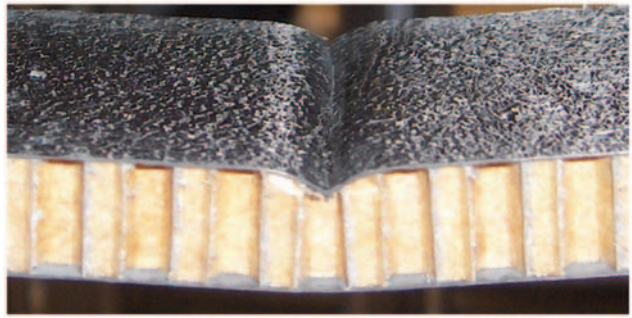

Figure 4. *Failure mode of the skin under compression. The skin became locally unstable and crushed the core.*

where u_f and w_f are the displacements in length and out-of-plane directions of the face, τ_{xz} the shear stress in the core, σ_z the normal stress in the core, A the coefficient A_{11} of the ABD matrix of the skin calculated according to classical laminate theory, D the bending stiffness of the skin, and N the in-plane load per unit width in the skin. The equilibrium equations of the core are given as:

$$\begin{aligned} w_c &= -\frac{z^2}{2E_c}\frac{d\tau_{xz}}{dx} + z\frac{k_1}{E_c} \qquad u_c = z\frac{\tau_{xz}}{G_c} + \frac{z^3}{6E_c}\frac{d^2\tau_{xz}}{dx^2} - \frac{z^2}{2E_c}\frac{dk_1}{dx} \\ \sigma_z &= -z\frac{d\tau_{xz}}{dx} + k_1 \end{aligned} \tag{2}$$

where k_1 is a coefficient function of x only, E_c is the core Young's modulus in z-direction, and G_c the core shear modulus in zx-direction. The shape of the skin was considered to be sinusoidal, and thus the shear stresses in the core, the normal stresses in the core, and the coefficient k_1 also had a sinusoidal form:

$$\begin{aligned} w_f &= W\sin\left(\frac{\pi x}{l}\right) \qquad \tau_{xz} = T_{xz}\cos\left(\frac{\pi x}{l}\right) \\ \sigma_z &= \Sigma_z\sin\left(\frac{\pi x}{l}\right) \qquad k_1 = K_1\sin\left(\frac{\pi x}{l}\right) \end{aligned} \tag{3}$$

where l is the half-wavelength of the wrinkling form. Assuming that the displacements at the top of the core are the same as in the middle of the skin (valid for thin skins), Equations (2) can be substituted in Equations (1). Suitable differentiation and substitution lead to a differential equation with only τ_{xz} as variable and, using the sinusoidal forms, we obtain the equation

$$q_1\left(\frac{\pi}{l}\right)^8 + q_2\left(\frac{\pi}{l}\right)^6 + q_3\left(\frac{\pi}{l}\right)^4 + q_4\left(\frac{\pi}{l}\right)^2 + q_5 = 0 \tag{4}$$

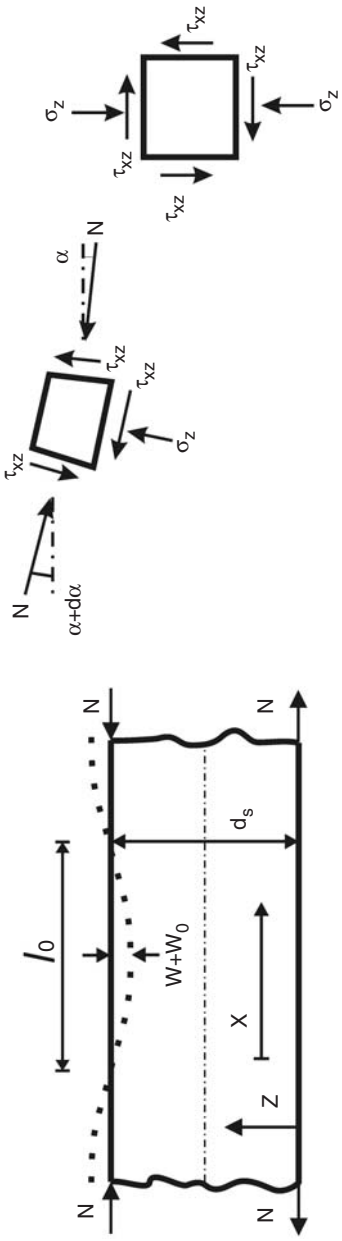

Figure 5. *Schematic view of the wrinkling phenomenon of the skin under compression during bending of the sandwich beam and of the stress on a skin element and a core element. The core is considered as a continuum. d_s is the distance between the center of the two faces, α is the angle between sandwich plane and the normal to the skin element.*

in which

$$q_1 = \frac{d_s^2 D}{6E_c} \quad q_2 = \frac{2d_s D}{G_c} - \frac{Nd_s^2}{6E_c} \quad q_3 = \frac{2D}{Ad_s} + \frac{2d_s}{3} - \frac{2N}{G_c}$$
$$q_4 = \frac{2E_c}{G_c d_s} - \frac{2N}{Ad_s} \quad q_5 = \frac{2E}{Ad_s^2} \tag{5}$$

By solving Equation (4), the wrinkling line load N in the face can be calculated as a function of l. The value of l, giving the lowest load, corresponds to the critical wavelength and gives the critical wrinkling load of the beam.

In order to take into account the adhesive layer used for core to skin bonding in the model, the bending stiffness of the skin was replaced by the bending stiffness of the skin with adhesive menisci, which was measured with the various adhesive weights.

This wrinkling formula is only valid for beams with perfectly flat skins. However, skins always contain imperfections. In particular, the waviness caused by vacuum bag processing changed the wrinkling load and had to be taken into account in the model. In fact, the initial deflection of the skin would increase during loading and could cause either compressive failure of the core, debonding of the skin, shear failure of the core, or local failure of the skin due to compression and bending deformations. The approach to taking the initial waviness into account was to consider that the skin had a sinusoidal shape of amplitude W_0, and a half-wavelength l_0, before loading, so that the deformed shape had the form

$$w_f + w_{f0} = (W_0 + W)\sin\left(\frac{\pi x}{l_0}\right). \tag{6}$$

The wavelength in Equation (6) was determined by the honeycomb geometry, and was not chosen arbitrarily to minimize N. With the honeycomb core, l_0 is the distance between two cells rows, i.e., 2.77 mm with 3.2 mm cell size and in ribbon direction. The amplitude of the waviness measured in the panels W_{meas} could not be used directly for W_0, because the wave measured had a width limited to the cell size, the skin being maintained flat on the cell walls, while the wave extended across the full width of the beam in the model. This discontinuity of the wave in the width direction would significantly reduce the sensitivity of the structure to waviness, and a factor $\theta = W_{meas}/W_0$ had to be identified in order to use the measured waviness in the model. The equilibrium Equations (1) for the skin become

$$A\frac{d^2 u_f}{dx^2} = (\tau_{xz})_{z=d_s} - D\frac{d^4 w_f}{dx^4} - N\frac{d^2 w_f}{dx^2} - N\frac{d^2 w_{f0}}{dx^2} = (\sigma_z)_{z=d_s} \tag{7}$$

By combining this with Equations (2), (3), and (7), one obtains the amplitude of shear stresses in the core τ_{xz}

$$\mathrm{T}_{xz} = \frac{NW_0(\pi/l_0)^5}{q_1(\pi/l_0)^8 + q_2(\pi/l_0)^6 + q_3(\pi/l_0)^4 + q_4(\pi/l_0)^2 + q_5}. \tag{8}$$

Then by using Equations (2), the amplitudes of the coefficient k_1 and of the normal stress in the core σ_z are:

$$\begin{aligned} K_1 &= \frac{2E_\mathrm{c}\mathrm{T}_{xz}}{Ad_\mathrm{s}^2}\left(\frac{l_0}{\pi}\right)^3\left(\frac{Ad_\mathrm{s}}{G_\mathrm{c}}\left(\frac{\pi}{l_0}\right)^2 - \frac{Ad_\mathrm{s}^3}{6E_\mathrm{c}}\left(\frac{\pi}{l_0}\right)^4 + 1\right) \\ \Sigma_z &= \mathrm{T}_{xz}d_\mathrm{s}\frac{\pi}{l_0} + K_1. \end{aligned} \tag{9}$$

With Equations (8) and (9) the critical load N causing shear stresses, or normal stresses, equal to the strength of the core can be calculated. The maximum local compressive strain in the face due to the compression and local bending of the face is:

$$\varepsilon_\mathrm{m} = \left(-\frac{\mathrm{d}^2 w_f}{\mathrm{d}x^2}\right)_\mathrm{m} h + \frac{N}{A_{11}} = W\frac{\pi^2}{l_0^2}h + \frac{N}{A_{11}} \tag{10}$$

where h is the distance from the neutral axis of the face to the most loaded fibers, i.e., 40.5 μm for the 0/90° laminate used. By setting this strain equal to the maximum compressive strain of the prepreg, the critical load can be determined for this failure type. The lowest of the loads calculated for the different types of failure is the critical load of the structure.

RESULTS

Influence of Adhesive Weight on Strength

The failure of the sandwich beams was always due to local instability of the skin crushing the core. No debonding occurred even with very low adhesive weight. However, the failure strength of the sandwich samples increased with adhesive weight. This can be explained by the increased size of the adhesive menisci on the skin, which significantly increased the bending stiffness, as shown on Figure 6. Owing to the geometry of the adhesive menisci, for a given adhesive quantity, the reinforcing effect was much more pronounced with menisci than with an even adhesive layer.

By inserting into the wrinkling model the relation between bending stiffness and the adhesive weight as determined in Figure 6, the critical wrinkling load and corresponding critical half-wavelength can be calculated as a function of adhesive weight in the menisci. The result is represented in Figure 7 and the critical load corresponded well to the experimental data, with errors smaller than 5%. The critical half-wavelength, which was calculated in the model by considering a continuous core, ranged from 2.3 to 3.2 mm, which is in fact close to honeycomb cell size. The elastic foundation was thus not continuous in the order of magnitude of the wavelength. However, a line in the width direction of the beam always crossed the same number of honeycomb cell

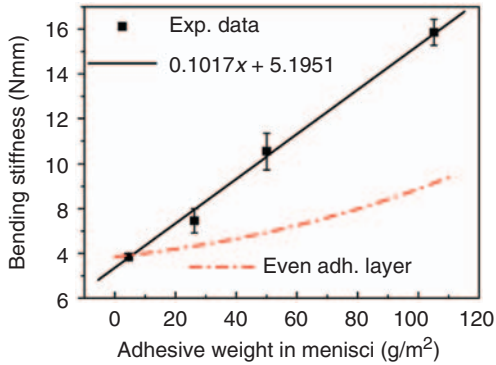

Figure 6. *Bending stiffness of the skin measured in three-point bending as a function of adhesive weight in the menisci for skin-to-core bonding. The theoretical stiffness calculated with CLT for an even adhesive layer is also represented.*

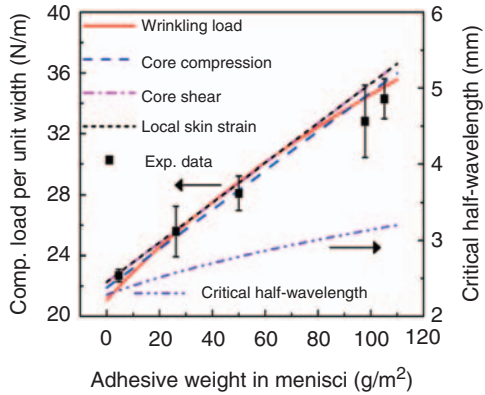

Figure 7. *Compressive load per unit width in the skin at failure under four-point bending, and critical half-wavelength for wrinkling as a function of adhesive weight in the menisci for core-to-skin bonding. The critical loads for the different types of failure are presented.*

walls, independently of the position in the length direction of the beam. The support of this line was therefore almost constant in the length direction, so that the properties of the foundation could be considered as constant in length direction, and the wrinkling model is thus still valid.

Even though the skin was cured against the Al plate, a slight initial waviness could not be completely avoided. Furthermore, as the half-wavelength of the preliminary deformation (2.77 mm) was close to the critical half-wavelength calculated for the wrinkling of perfectly flat skin, the initial waviness strongly influenced the strength of the beam. An arbitrary small waviness $W_0 = 0.5\,\mu m$ was used to calculate the critical loads for core compressive and shear stresses, and local strains in the skin. With this small initial deformation, the failure loads for all three models were very close to the calculated wrinkling load and are presented in Figure 7. Predicted loads for shear failure of the core and local compressive failure of the skin were identical and greater than the failure load for core compressive failure, which was close to the wrinkling load. The failure mode is thus a coupling between local skin instability and core compressive failure, which is confirmed by observation of the broken sample illustrated in Figure 4. Hence, when the skin under compression is very smooth, the failure load can be predicted accurately either by the wrinkling model or by considering a small initial imperfection causing compressive failure of the core, and by taking into account the stiffening effect of the adhesive menisci on the skins.

Influence of Process Pressure on Microstructure

Figures 8 and 9 show cross-sections of samples cured respectively in two steps and in one shot with relative pressure in the vacuum bag ranging from -0.1 to -0.9 bar. Figure 10 shows the measured adhesive weight in the menisci and the waviness amplitude as a function of process pressure. It is important to remember that the pressure shown is the relative pressure in the vacuum bag. However, the actual absolute pressure in the honeycomb cells may be significantly higher than the absolute pressure in the vacuum bag during one-shot curing due to the low permeability of the skins and consumables used. The interplay between process pressure, skin waviness, and adhesive weight in menisci is evident. Both waviness and adhesive weight increased when the relative pressure in the vacuum bag diminished. The increase was less pronounced for the samples cured in one shot because the vacuum was not good in the honeycomb cells due to low permeability of the lay-up, as explained previously. As the waviness should be 0 when no pressure was applied, the data were fitted with either a power law of the pressure applied, or a linear fit, as illustrated in Figure 10.

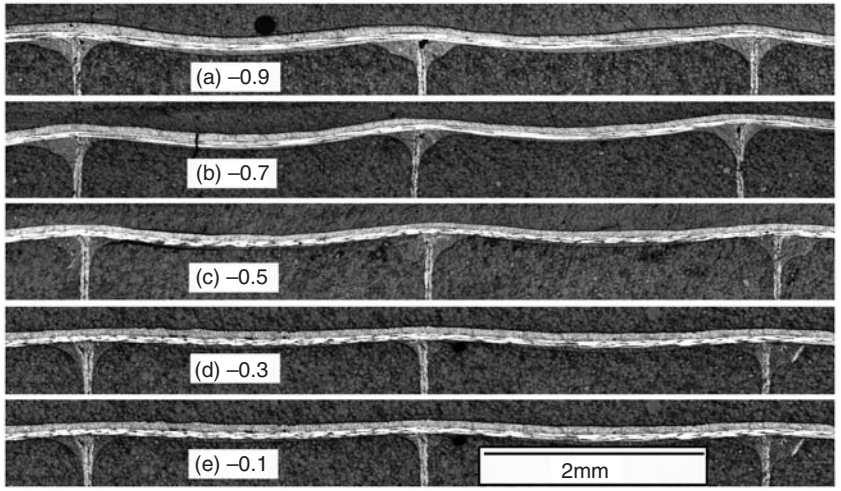

Figure 8. *Micrographs of cross sections of the wavy side of sandwich panels cured in two steps. The skin laying on three honeycomb cell walls and bonded with adhesive menisci can be observed. The relative pressures applied during vacuum curing were −0.9, −0.7, −0.5, −0.3 and −0.1 bar.*

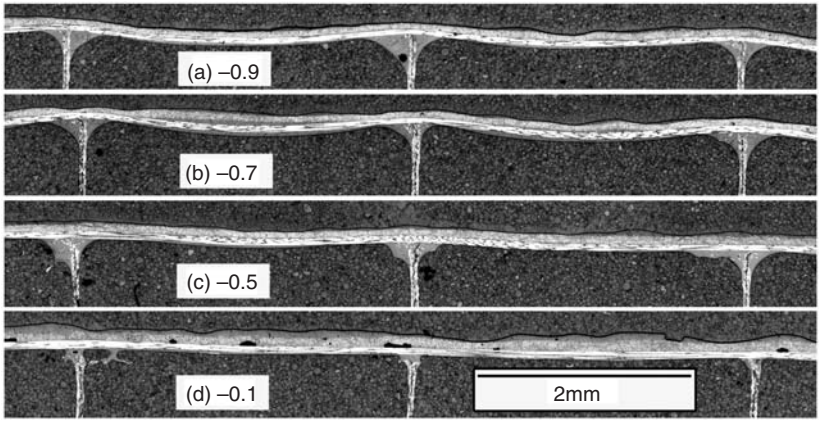

Figure 9. *Micrographs of cross sections of the wavy side of sandwich panels cured in one shot. The relative pressures applied during vacuum curing were −0.9, −0.7, −0.5 and −0.1 bar.*

For the samples cured in two steps, the size of the adhesive menisci forming between core and skin increased between −0.1 and −0.3 bar pressure in the vacuum bag, and then stabilized. When pressure was exerted by the honeycomb cell wall, the skin was compacted under the honeycomb cell wall and prepreg resin flowed into the menisci, in addition to the 50 g/m^2

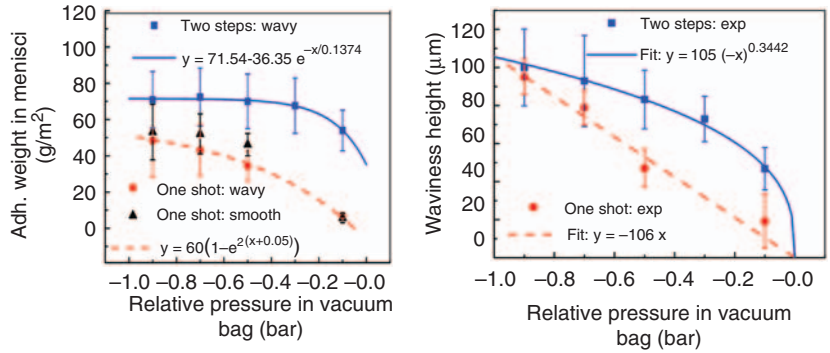

Figure 10. *Adhesive weight in the menisci (left) and height of the waviness W_{meas} (right) measured on cross-sections as a function of process pressure for the samples cured either in two steps or in one shot.*

of adhesive film. As the amount of resin was limited, the meniscus size did not change above a sufficient pressure level. When low pressure was applied, the menisci only formed with the adhesive film near the cell wall. For the samples cured in one shot, the menisci were almost inexistent at −0.1 bar relative pressure in the vacuum bag. This was due to bad air circulation in honeycomb cells closed by the two skins, causing the pressure to increase when temperature rose. Some air flowed out of the cells through the skin and forced adhesive and prepreg resin to flow out. This can be seen in Figure 9(d) where a layer of resin is on the top of the prepregs of the panel cured with −0.1 bar relative pressure in the vacuum bag. This flowing effect was more pronounced on the vacuum bag side that on the Al mould, what explains why the resin fillets were greater on the mold side than on the vacuum bag side, as shown in Figure 10. To fit the data by taking into account the limited amount of adhesive available, functions starting with a finite adhesive weight growing asymptotically to the limit adhesive quantity were chosen, and first-order exponential decay functions were used as illustrated in Figure 10.

Influence of Process Pressure on Strength

Figure 11 shows the strength of the panels manufactured with various vacuum pressures and tested in four-point bending. Interestingly, at first, when the relative pressure in the vacuum bag was decreased, the strength of the beams increased, then reached a maximum and finally decreased. The same behavior was observed for the panels cured in two steps and in one shot, only in this case the maximum strength was obtained at different pressures, respectively −0.3 and −0.7 bar relative pressure in the vacuum bag.

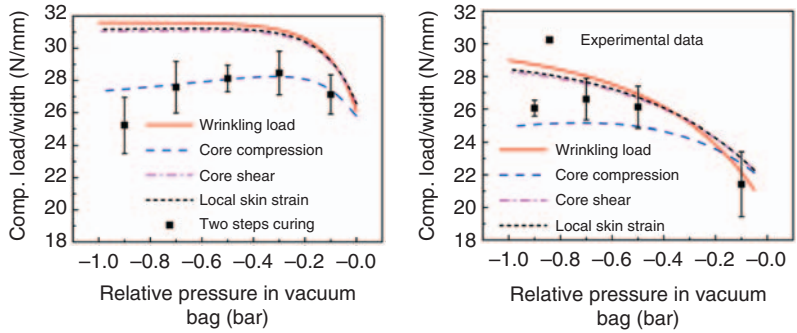

Figure 11. *Changes in the compressive load per unit width in the facesheet at failure during four-point bending tests as a function of process pressure for the samples cured in two steps (left) and in one shot (right).*

The strength increase was due to the rapid increase of adhesive quantity in menisci when relative pressure in the vacuum bag decreased. Then the adhesive quantity stabilized and the increasing waviness of the skin decreased the strength of the face. The maximum strength of the panels cured in two steps was slightly higher than for panels cured in one shot. This was due to the greater size of the adhesive menisci obtained during two-step curing, as was observed in Figure 10.

In order to take into account the discontinuity of waviness in the width direction of the beam in the model, which significantly reduced the sensitivity to initial waviness, the factor $\theta = W_{\text{meas}}/W_0$ was determined to be 25 by adjusting the model to the experimental data obtained with the panels cured in two steps. Figure 11 shows changes in the critical compressive load per unit width in the skin calculated by using the models adapted to the different types of failure as a function of the process pressure. Among the models predicting the different possible failure types of the skin under compression, the one that considers compressive failure of the core gave the lowest failure load. Thus, this mode was the most sensitive to the initial imperfections of the skin and therefore determined the failure load of the beam. Using the previously defined parameter, θ, the model giving the critical load for core compressive failure was in good agreement with the experimental data with errors of $<5\%$ for both the panels cured in two steps or in one shot. For the panels cured in one shot, the model slightly overestimated the failure load at -0.1 bar relative vacuum pressure, due to bad compaction of the skin at low pressure, which was not accounted for. Furthermore, the curve showing the critical load for core compressive failure replicated exactly the same tendencies as the experimental data, with the load increasing rapidly at first when relative vacuum pressure decreased, then reaching a maximum, and finally decreasing. The model confirmed the

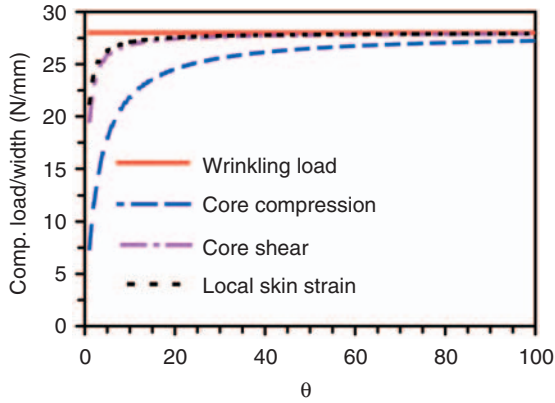

Figure 12. *Influence of the factor θ on the failure loads predicted with the different models, calculated for one shot curing with −0.7 bar relative pressure in vacuum bag.*

existence of an optimum process pressure controlled by the interplay between skin waviness and the formation of adhesive menisci at the skin–honeycomb interface. The model and the experimental data for wavy skin gave the same optimal pressure in the vacuum bag for the sandwich panels cured in two steps at about −0.3 bar. The optimal pressure for the panels cured in one shot was around −0.7 bar, but the strength did not change significantly between −0.5 and −0.9 bar. Finally, the critical failure mode, predicted by the model as being the compressive failure of the core, was confirmed by observing the broken samples where the skin crushed the core, as illustrated in Figure 4.

It is also interesting to observe the sensitivity of the model to the parameter θ as detailed in Figure 12. Of course the wrinkling load, which does not consider waviness of the skin, is not affected by the choice of θ. The failure load predicted by the other models is too low when no correction of the measured waviness is made ($\theta = 1$), i.e., if the waviness prior to loading is perfectly sinusoidal and not limited to cell size. The failure loads increase then quickly with the stabilization factor θ and tend asymptotically toward the wrinkling load. It confirms that the models converge toward wrinkling load when waviness can be neglected.

As the predictions of the model with selected θ value correlated well to the experimental data, these can then be used to predict what happens if supplementary pressure is added during one-shot curing by using an autoclave. The predicted failure load is represented in Figure 13 as a function of the process pressure, i.e., the pressure difference between outside and inside the vacuum bag. At two-bar pressure (−0.9 bar relative pressure in the vacuum bag and 1.1 bar relative pressure in the autoclave), the strength of the

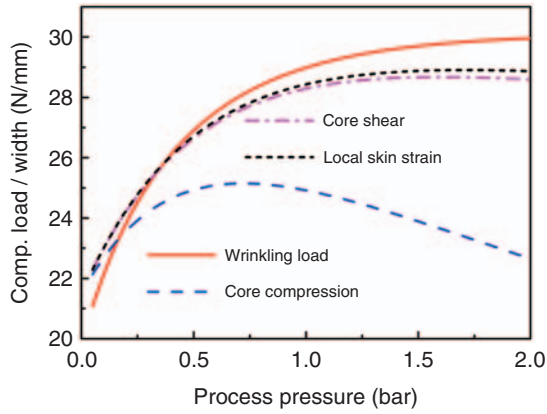

Figure 13. *Changes in the compressive load per unit width in the facesheet at failure for a sandwich cured in one shot, during a four-point bending test with the wavy face under compression, as a function of process pressure.*

beam would be reduced by 10% compared with optimal pressure, even though the model did not take into account any damage caused to the honeycomb by high processing pressure. The model confirmed that the use of supplementary pressure with sandwich structures with light cores and thin skins decreased their properties and should therefore be avoided.

CONCLUSIONS

The bending strength of ultralight sandwich structures (700–800 g/m^2) is very sensitive to the process pressure used during manufacturing. By using vacuum bag processing with various pressures and adhesive weights, it was shown that the waviness of the skin and the size of the adhesive menisci forming between honeycomb cell walls and skins have a direct influence on the wrinkling strength of the skin. During one-shot vacuum bag curing, the waviness of the skin and the size of the adhesive menisci both increased with process pressure, thereby exerting opposing effects on the strength. An optimal process pressure was identified at −0.7 bar relative pressure in the vacuum bag. This pressure was clearly related to the materials used, and also to the curing cycle parameters, a higher temperature creating for example a higher pressure in the honeycomb cells.

A model was developed to predict the wrinkling load of the skin as a function of process pressure by taking into account the influence of adhesive weight in the menisci and the waviness of the skin. Good agreement was found between experimental data and the model which contributed to a better understanding of the failure mechanisms controlling wrinkling load.

The model demonstrated that the use of higher process pressure during curing using an autoclave would decrease the strength and should thus be avoided with such ultra-light sandwich structures.

ACKNOWLEDGMENTS

The authors wish to acknowledge the EPFL and Swiss Innovation Promotion Agency (CTI, #8002.1, DCPP-NM) for financial support.

REFERENCES

1. Funke, H. (2001). Systematische entwicklung von ultra-leichtbaukonstruktionen in faserverbund-wabensandwichbauweise am beispiel eines kleinflugzeuges, PhD Thesis, Universität-GH Paderborn.
2. Funke, H. (2004). Development of the Ultralight Aircraft Silence, *JEC – Composites*, **10**: 52–54.
3. Middleton, D.H. (1990). Composite Materials in Aircraft Structures, Longman Harlow, London.
4. Rozant, O., Bourban, P.E. and Månson, J.A.E. (2001). Manufacturing of Three Dimensional Sandwich Parts by Direct Thermoforming, *Composites Part A: Applied Science and Manufacturing*, **32**(11): 1593–1601.
5. Baldock, N. and Mokhtarzadeh-Dehghan, M.R. (2006). A Study of Solar-powered, High-altitude Unmanned Aerial Vehicles, *Aircraft Engineering and Aerospace Technology*, **78**(3): 187–193.
6. Cestino, E. (2006). Design of Solar High Altitude Long Endurance Aircraft for Multi Payload & Operations, *Aerospace Science and Technology*, **10**(6): 541–550.
7. Romeo, G., Frulla, G., Cestino, E. and Corsino, G. (2004). Heliplat: Design, Aerodynamic, Structural Analysis of Long-endurance Solar-powered Stratospheric Platform, *Journal of Aircraft*, **41**(6): 1505–1520.
8. Triantafillou, T.C. and Gibson, L.J. (1987). Minimum Weight Design of Foam Core Sandwich Panels for a Given Strength, *Materials Science and Engineering*, **95**: 55–62.
9. Triantafillou, T.C. and Gibson, L.J. (1987). Failure Mode Maps for Foam Core Sandwich Beams, *Materials Science and Engineering*, **95**: 37–53.
10. Ley, R.P., Lin, W. and Mbanefo, U. (1999). *Facesheet Wrinkling in Sandwich Construction*, NASA Langley Research Center, Hampton, VA, USA.
11. Thomsen, O.T. and Banks, W.M. (2004). An Improved Model for the Prediction of Intra-cell Buckling in CFRP Sandwich Panels under In-plane Compressive Loading, *Composite Structures*, **65**(3–4): 259–268.
12. Gdoutos, E.E., Daniel, I.M. and Wang, K.A. (2003). Compression Facing Wrinkling of Composite Sandwich Structures, *Mechanics of Materials*, **35**(3): 511–522.
13. Norris, C.B., Boller, K.H. and Voss, A.W. (1953). Wrinkling of the Facings of Sandwich Construction Subjected to Edgewise Compression, Sandwich Construction having Honeycomb Cores, Forest Products Laboratory, Wisconsin.
14. Hoff, N.J. and Mautner, S.E. (1945). The Buckling of Sandwich-type Panels, *Journal of the Aeronautical Sciences*, **12**(3): 285–297.
15. Yusuff, S. (1955). Theory of Wrinkling in Sandwich Construction, *Journal of the Royal Aeronautical Society*, **59**(529): 30–36.

16. Kassapoglou, C., Fantle, S.C. and Chou, J.C. (1995). Wrinkling of Composite Sandwich Structures Under Compression, *Journal of Composites Technology & Research*, **17**(4): 308–316.
17. Fagerberg, L. and Zenkert, D. (2005). Imperfection-induced Wrinkling Material Failure in Sandwich Panels, *Journal of Sandwich Structures & Materials*, **7**(3): 195–219.
18. Allen, H.G. (1969). *Analysis and Design of Structural Sandwich Panel*, Pergamon Press, Oxford.
19. Altstadt, V., Diedrichs, F., Lenz, T., Bardenhagen, H. and Jarnot, D. (1998). Polymer Foams as Core Materials in Sandwich Laminates (Comparison with Honeycomb), *Polymers & Polymer Composites*, **6**(5): 295–304.
20. Rion, J., Geiser, A., Leterrier, Y. and Månson, J.-A.E. (2006). Ultralight Composite Sandwich Structure: Optimization of Skin to Honeycomb Core Bonding, In: *Proceedings of 27th International Conference of SAMPE Europe*, Paris.
21. Gutierrez, A.J. and Webber, J.P.H. (1980). Flexural Wrinkling of Honeycomb Sandwich Beams with Laminated Faces, *International Journal of Solids and Structures*, **16**(7): 645–651.
22. Rion, J., Demarco, F., Leterrier, Y. and Månson, J.-A.E. (2007). Damage Analysis of Ultralight Sandwich Structures, In: *Proceedings of ICCM16, 16th International Conference on Composite Materials*, Japan.
23. Rion, J., Leterrier, Y. and Månson, J.-A.E. (2008). Prediction of the Adhesive Fillet Size for Skin to Honeycomb Core Bonding in Ultra-light Sandwich Structures, *Composite Part A*, **39**(9): 1547–1555.